

Modelling shows that, positive of the pitting potential, chromate ion is associated with a large pseudo-capacitance of the order of  $150\mu\text{F cm}^{-2}$ , clear from the low-frequency variation. At these potentials, nitrite ion does not inhibit the corrosion process.

Scanning electron microscopy of the surfaces of the aluminium electrodes submitted to an applied potential of  $-0.5\text{V}$  vs. SCE for 20 minutes showed crystallographically etched pits for chloride and for chloride plus nitrite solutions, but no visual evidence of pitting for chromate-containing solutions. Thus, this and the impedance results point to the strong adsorption of chromate ion at potentials positive of the pitting potential and its aiding oxide growth and repair of defects in the oxide film, probably through reduction of the chromate ion with simultaneous production of oxide ions.

In conclusion, the inhibitor action for both these anions has been demonstrated and both of them adsorb and compete with chloride ion on the aluminium surface. At potentials more negative than the pitting potential, nitrite is the more effective inhibitor, but this situation is reversed at more positive potentials, due to the ability of chromate ion to aid oxide film growth. Of the electrochemical techniques employed, impedance is that which gives most information about the electrode processes occurring.

#### REFERENCES

1. C.M.A. Brett, *Corrosion Sci.*, 1992, **33**, 203 and references therein.
2. G. Trabanelli, *Corrosion*, 1991, **47**, 410.
3. A.M. Shams El Din and N.J. Paul, *Thin Solid Films*, 1989, **189**, 205.
4. J.W. Schültze, M.H. Lohrengel and D. Ross, *Electrochim. Acta*, 1983, **28**, 973.

#### A VOLTAMMETRIC STUDY OF SILVER DEPOSITION ON CARBON MICROELECTRODES

J.P. Sousa

FEUP/ Departamento de Eng<sup>a</sup> Química

Rua dos Bragas, 4099 Porto Codex

PORTUGAL

The development of microelectrodes has made an impact in the electrochemistry domain, opening up new opportunities for the investigation of in situ properties of several systems. This has led to the evolution of a major number of theoretical methods which model the properties of such systems. Due to the high quality and precision of the experimental data acquired with microelectrodes novel concepts have been achieved and hitherto inaccessible parameters have been determined.

It has been shown elsewhere [1] that it is possible to obtain a complete description of the single and double potential step experiments associated to the metallic nucleation process. The basic reason why it is possible to do this is that the time dependence of the radius can be determined.

Linear sweep voltammetry (LSV) measurements have the advantage that they traverse the whole range of potentials. The disadvantage is that one cannot obtain a complete closed form analytic description of the experiments. The reason is that it seems impossible to integrate the non-linear inhomogeneous expression

$$\frac{dr}{dt} = \frac{Mk_{Ag^+}}{\rho} = \frac{Mk_{Ag^+}^0}{\rho} \frac{\left\{ \exp\left(\frac{-\alpha_{Ag^+}Fv t}{RT}\right) - \exp\left(\frac{(1-\alpha_{Ag^+})Fv t}{RT}\right) \right\}}{\left\{ 1 + \frac{rk_{Ag^+}^0}{D_{Ag^+}C_{Ag^+}^\infty} \exp\left(\frac{-\alpha_{Ag^+}Fv t}{RT}\right) \right\}} \quad (1)$$

where  $r$  (cm) is the radius of the particle,  $t$  (s) is the time,  $K_{Ag^+}$  and  $K_{Ag^+}^0$  ( $\text{mols cm}^{-2}\text{s}^{-1}$ ) are rate constants of crystal growth,  $M$  ( $\text{g mol}^{-1}$ ) is the molecular weight,  $\rho$  ( $\text{g cm}^{-3}$ ) is the density,  $\alpha_{Ag^+}$  are the transfer coefficients,  $v$  ( $\text{V s}^{-1}$ ) is the potential sweep rate,  $C_{Ag^+}^\infty$  ( $\text{mol cm}^{-3}$ ) is the bulk concentration,  $T$  ( $^\circ\text{C}$ ) is the temperature,  $D_{Ag^+}$  ( $\text{cm}^2 \text{s}^{-1}$ ) is the diffusion coefficient and  $F$  ( $\text{C mol}^{-1}$ ) is the Faraday constant. It is only possible to do this numerically and, in such numerical procedures, one can be guided by the parameters established for the potentiostatic experiments. So far, theoretical simulations were drawn for the two limiting conditions, i.e., diffusion controlled growth and kinetically controlled deposition [1].

The general form of the current-time relationship will be

$$I = 2\pi z F k_1(t) [r(t)]^2 \quad (2)$$

$$= 2\pi z F \frac{k_1^0 \left[ \exp\left(\frac{-\alpha_1 F \nu t}{RT}\right) - \exp\left(\frac{(1-\alpha_1) F \nu t}{RT}\right) \right] [r(t)]^2}{\left[ 1 + \frac{k_1^0 [r(t)]}{D_1 C_1^\infty} \exp\left(\frac{-\alpha_1 F \nu t}{RT}\right) \right]}$$

where it has been assumed that the growing centre is a hemisphere with area  $2\pi[r(t)]^2$  [2]. All the information about the effects of induction times,  $t_0$ , and the cathodic limit,  $t_1$ , is contained in  $r(t)$ . The term  $\nu t$  in equation (2) is simply the instantaneous value of the overpotential.

Experimentally,  $r(t)$  is determined by integrating the current-time transient (peak-shaped voltammogram). It is more convenient to rearrange equation (2) into a different form which gives more useful information

$$\frac{I(t)}{2\pi z F [r(t)]^2 \left[ 1 - \exp\left(\frac{F \nu t}{RT}\right) \right]} = \frac{k_1^0 \exp\left(\frac{-\alpha_1 F \nu t}{RT}\right)}{\left[ 1 + \frac{k_1^0 [r(t)]}{D_1 C_1^\infty} \exp\left(\frac{-\alpha_1 F \nu t}{RT}\right) \right]} \quad (3)$$

and this can be further rearranged into

$$\left\{ \frac{2\pi z F [r(t)]^2}{I(t)} \left[ 1 - \exp\left(\frac{F \nu t}{RT}\right) \right] - \frac{r(t)}{D_1 C_1^\infty} \right\} = \frac{1}{k_1^0} \exp\left(\frac{\alpha_1 F \nu t}{RT}\right) \quad (4)$$

where for any experimental systems, all the parameters in the left hand side (LHS) are known. Therefore a plot of the natural logarithm of the LHS term versus  $\nu t$  gives a fairly conventional Tafel plot [3]. From the slope, the value of  $\alpha$  is obtained while the extrapolation to  $\eta = 0$  gives  $\ln(1/K^0)$  and hence  $K^0$ . Such procedure has been applied to analyse the voltammogram shown in Fig.1. The values obtained were  $\alpha = 0.4$  and  $K_0 = 3.7 \cdot 10^{-7} \text{ mol.cm}^{-2} \cdot \text{s}^{-1}$ .

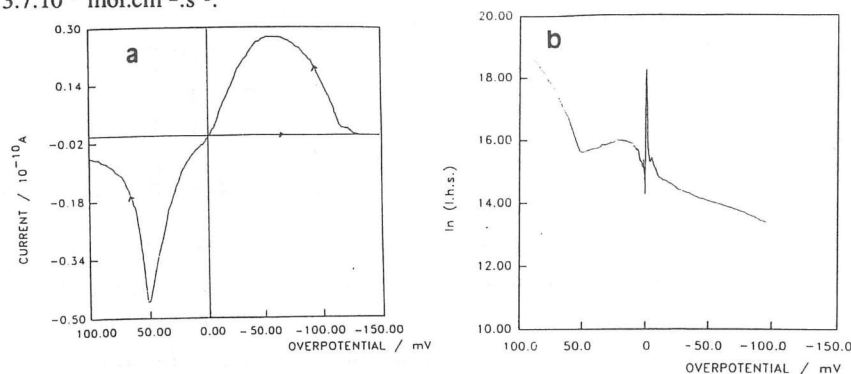


Figure 1 Linear sweep voltammogram for the deposition of silver onto vitreous carbon microdisk electrode from 5.0 mM  $\text{AgNO}_3$  in aqueous  $\text{KNO}_3$ ;  $\nu = 100 \text{ mV/s}$ ;  $I = 0.005 \text{ nA/cm}$  (a): (b) Tafel plot of the voltammogram.

A theoretical simulation using these values is presented in Fig.2. This shows that indeed the cathodic branch can be fitted quite accurately but the anodic branch presents significant deviations. A possible explanation of the observed behaviour is that during the stripping process there is some kind of film formation at the substrate surface which narrows the current transient and sharpens the dissolution peak. It also shows that several other parameters need to be accounted for in order to obtain a closer fit between theoretical and experimental plots.

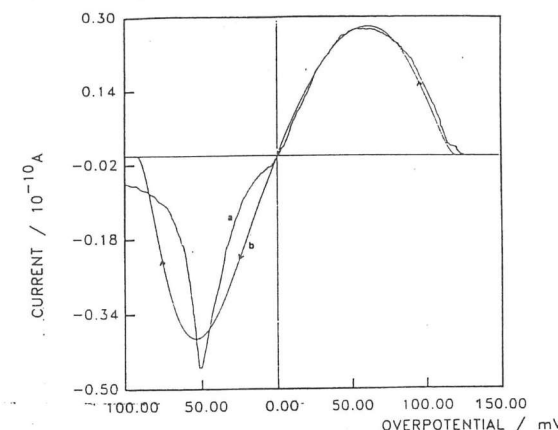


Figure 2 Plot of the linear sweep voltammograms for the silver deposition: a) experimental; b) calculated using  $\alpha = 0.4$ ,  $z = 1$  and  $K^0 = 3.7 \cdot 10^{-7} \text{ mol cm}^{-2} \text{ s}^{-1}$ , equation (2).

Since the experimental voltammograms cannot be represented by either diffusion or kinetic control, theoretical simulations must be used based on equation (1). Fig. 3 illustrates the same kind of plot but making  $z = 2$  instead of 1 and using smaller values for  $K^0$  and  $\alpha$ . It is clear that the fit between experimental and theoretical plots has improved on the anodic branch but the opposite is true for the cathodic branch. Therefore, a compromise between these two plots would fit the experimental voltammograms more closely.

The experimental evidence points to the fact that the lattice formation is more complicated than the mechanism that has been assumed [4]:



Furthermore, the differences between the experimental and calculated values can be interpreted in terms of a decrease of  $K^0$  with time due to a decrease in the number of

lattice forming sites per unit area of the growth centre which could be caused by the development of a faceted crystal bounded by low index faces.

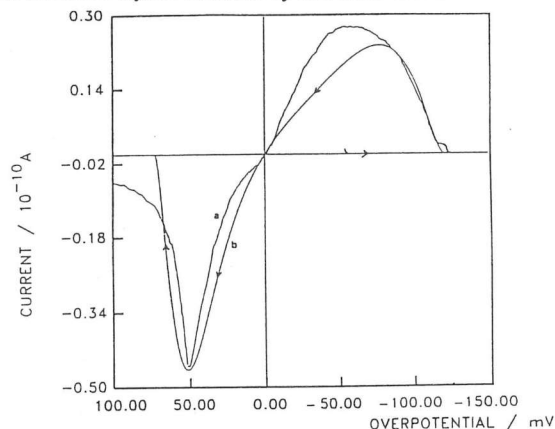


Figure 3 Plot of the linear sweep voltammograms for the silver deposition: a) experimental; b) calculated using  $\alpha = 0.35$ ,  $z = 2$  and  $K^0 = 1.2 \cdot 10^{-7} \text{ mol cm}^{-2} \text{ s}^{-1}$ , equation (2).

In summary one can say that attempts to interpret the experimental evidence observed for the silver LSV measurements points out to kinetic complexities associated to the silver crystallisation process and that these studies have so far been restricted to a rather narrow range of conditions mainly because of the restrictions posed by the mathematical analysis.

### References

1. J.P. Sousa, Ph.D. Dissertation, University of Utah, 1991.
2. K.B. Oldham, *J. Electroanal. Chem.*, **122** (1981) 1.
3. *Instrumental Methods in Electrochemistry: Southampton Electrochemistry Group*, (Eds.) R. Greef, R. Peat, L.M. Peter, D. Pletcher and J. Robinson, John Wiley & Sons Publishers, New York (1985)
4. G. Gunawardena, G. Hills and I. Montenegro, *Electrochim. Acta*, **23** (1987) 693.

### RESPOSTAS VOLTAMÉTRICAS DO IRÍDIO: REDUÇÃO DO INTERVALO DE POLARIZAÇÃO E EFEITO DO ANIÃO

M. Teresa C. Portela, M. Irene S. Lopes e Inês T.E. Fonseca  
CECUL, Departamento de Química - Faculdade de Ciências,  
Universidade de Lisboa, 1294 Lisboa Codex

The effects of cycling continuously the potential of an Ir electrode, between the  $\text{H}_2$  and  $\text{O}_2$  evolution reactions, in aqueous solutions of two different electrolytes, namely of  $\text{H}_2\text{SO}_4$  and  $\text{HClO}_4$  are reported.

Some peculiarities observed in the hydrogen adsorption desorption region, not previously reported are presented.

The observed effects promoted by the nature of the electrolyte are explained considering the specific and superequivalent adsorption of the  $\text{HSO}_4^-/\text{SO}_4^{2-}$  and  $\text{ClO}_4^-$  anions.

Os filmes de óxidos de irídio resultantes de polarizações cíclicas sucessivas, no intervalo de potencial delimitado pelas reacções de evolução do hidrogénio e oxigénio têm revelado elevada actividade electrocatalítica para a reacção de evolução do  $\text{O}_2$  [1-2]. Estudos visando a caracterização dos referidos filmes têm sido realizados por vários investigadores, em particular, pelos que se interessam por electrocatálise. Por essa razão iniciámos estes estudos.

Estabeleceram-se metodologias para a remoção de filmes espessos do eléctrodo de irídio e estudou-se a influência da natureza e concentração do electrólito na cinética do crescimento dos referidos filmes [3,4].

No presente trabalho pretende-se concluir sobre a influência do anião do electrólito e da redução do intervalo de polarizabilidade na resposta voltamétrica do irídio a polarizações cíclicas sucessivas.

São considerados as interfaces  $\text{Ir}/0.5\text{M H}_2\text{SO}_4$  e  $\text{Ir}/1\text{M}$